ACS APPLIED MATERIALS & INTERFACES

Research Article

www.acsami.org

Improved Electrochemical Performance of $LiCoO_2$ Electrodes with ZnO Coating by Radio Frequency Magnetron Sputtering

Xinyi Dai, Liping Wang,* Jin Xu, Ying Wang, Aijun Zhou, and Jingze Li*

State Key Laboratory of Electronic Thin Films and Integrated Devices, School of Microelectronics and Solid-State Electronics, University of Electronic Science and Technology of China, Chengdu 610054, China

Supporting Information

ABSTRACT: Surface modification of $LiCoO_2$ is an effective method to improve its energy density and elongate its cycle life in an extended operation voltage window. In this study, ZnO was directly coated on as-prepared $LiCoO_2$ composite electrodes via radio frequency (RF) magnetron sputtering. ZnO is not only coated on the electrode as thin film but also diffuses through the whole electrode due to the intrinsic porosity of the composite electrode and the high diffusivity of the deposited species. It was found that ZnO coating can significantly improve the cycling performance and the rate capability of the $LiCoO_2$ electrodes in the voltage range of 3.0−4.5 V. The sample with an optimum coating thickness of 17 nm exhibits an initial discharge capacity of 191 mAh g^{-1} at 0.2 C, and the capacity retention is 81% after 200 cycles. It also delivers superior rate performance with a reversible capacity of 106 mAh g^{-1} at 10 C. The enhanced cycling performance and rate capability are attributed to the stabilized phase structure and improved lithium ion diffusion coefficient induced by ZnO coating as evidenced by X-ray diffraction, cyclic voltammetry, respectively.

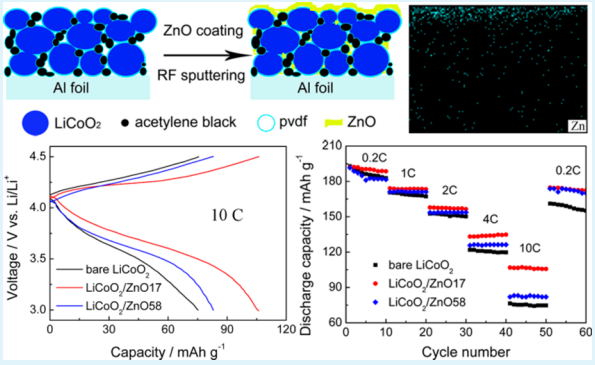

KEYWORDS: *lithium cobalt oxide, zinc oxide coating, RF magnetron sputtering, structure stability, lithium ion diffusion coefficient*

1. INTRODUCTION

Layered $LiCoO_2$ has been widely used as a cathode material for commercial lithium-ion batteries due to its favorable rate capability, excellent capacity retention, and high theoretical specific capacity. This cathode is typically charged up to 4.2 V vs Li/Li^+, and its corresponding discharge capacity is only around 137 mAh g^{-1}, which is much lower than its theoretical capacity of 274 mAh g^{-1}. It is well-known that higher capacity can be reached by simply extending the upper limitation electrode voltage over 4.2 V vs Li/Li^+. However, this will lead to severe structural degradation due to an irreversible hexagonal-monoclinic-hexagonal phase transition,[1−4] as well as a surface reaction with the electrolyte at a high oxidation state,[5,6] resulting in poor cycling performance.

A variety of efforts have been made to improve high-voltage cycling performance of $LiCoO_2$, including surface modification,[7−11] nanocrystallization,[12] and element such as Al,[13,14] Zn,[15] Mg,[16] and Fe.[17] Among them, surface coating is considered to be the most effective method without the sacrifice of specific capacity. There are many coatings, such as binary oxides (e.g., Al_2O_3,[18,19] ZnO,[7,20] ZrO_2,[21,22] MgO,[23] SnO_2,[24] and TiO_2[21,25]), metal phosphates (e.g., $AlPO_4$[26]), and metal fluorides (e.g., LiF[27,28] and MgF[29]). ZnO has been recognized to be a proper material for improving the cycling stability of layered $LiCoO_2$ cathodes at high cutoff voltages.[7,20] In a previous study, Fang et al.[20] claimed that ZnO coating can suppress the formation of passivating films on the $LiCoO_2$ surfaces, thus minimizing the growth of cathode impedance. Chang et al.[7] suggested that the improved capacity retention of ZnO-coated $LiCoO_2$ is due to the suppression of cation dissolution from the cathodes. Park et al.[30] suggested that ZnO scavenges HF, which is harmful to the electrochemical performance of cathodes. It should be noted that ZnO coating has previously been performed on loose $LiCoO_2$ particles. But because ZnO is a poor electronic conductor, the coating layer blocks the electronic transport, which impedes the kinetic behavior, especially at high current density.[18,31]

Recently, the application of coatings to fabricated electrodes rather than loose powders of the electrochemically active material has become a popular method of surface modification.[9,12,32−36] Directly coating the as-prepared composite electrodes may preserve the electronic transport pathways, since the interparticle, particle to current collector, and particle to carbon black contact points are still preserved. This method of surface modification may thus allow coating even with electronically insulating materials. Atomic layer deposition (ALD) is the most commonly employed deposition technique as a conformal coating layer with atomic-level thickness can be formed via physical/chemical adsorption on each component throughout the whole electrode.[37] However, ALD is a relatively

Received: May 25, 2014
Accepted: August 26, 2014
Published: August 26, 2014

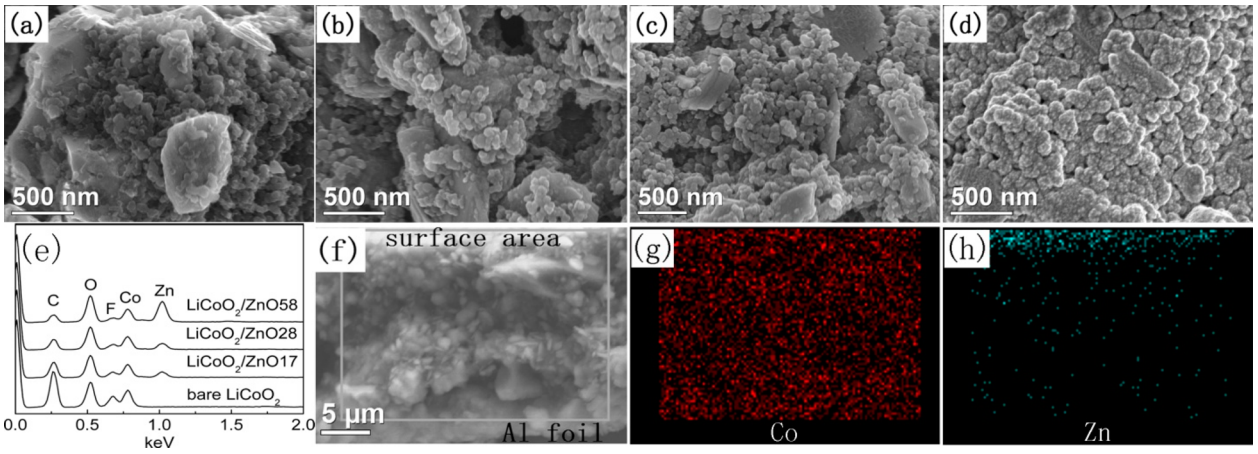

Figure 1. SEM images and EDS analysis of bare $LiCoO_2$ and $LiCoO_2$/ZnO*x* electrodes. SEM images of (a) bare $LiCoO_2$, (b) $LiCoO_2$/ZnO17, (c) $LiCoO_2$/ZnO28, and (d) $LiCoO_2$/ZnO58; (e) EDS curves of bare and $LiCoO_2$/ZnO*x* electrodes; (f) cross-sectional SEM image; and EDS maps for (g) Co element and (h) Zn element of $LiCoO_2$/ZnO17 sample.

complex process with low precursor material utilization efficiency and high cost, making it incompatible with the requirement of mass production.

In this study, we introduce a relatively economical and facile approach toward the application of ZnO thin-films to as-prepared $LiCoO_2$ composite electrodes using radio frequency (RF) magnetron sputtering. A conformal protective ZnO coating layer can also be realized not only on the electrode surface but also inside the porous composite electrode using this approach. The latter might be attributed to the high momentum of the plasma induced by the high radio frequency and high electric field. The crystal structure of $LiCoO_2$ is well maintained during the coating process. This surface-modified $LiCoO_2$ presents superior rate performance in a broad voltage window of 3.0−4.5 V vs Li/Li^+ with a reversible capacity of 106 mAh g^{-1} at 10 C. The effects of the ZnO thin coating layer on the electrode structure, charge transport properties, and electrochemical performance were systematically investigated.

2. EXPERIMENTAL SECTION

2.1. ZnO RF Magnetron Sputtering on $LiCoO_2$ Electrodes. ZnO films were directly grown on as-prepared $LiCoO_2$ electrodes (~20 μm thick, as a substrate) by RF (13.56 MHz) magnetron sputtering using a ZnO target (99.99%). Before sputtering, the substrate was heated to 110 °C to facilitate the removal of residual oxygen adsorbed on the substrate, and this temperature was maintained during the whole sputtering process. RF magnetron sputtering was performed with different depositions time to control the coating thickness, while the pressure and power were fixed at 0.5 Pa and 80 W, respectively. High purity (99.999%) argon was used as the working gas with the base pressure of less than 6.0×10^{-4} Pa. The target-to-substrate distance was set constant at 5.0 cm. The target was presputtered for 5 min to clean its surface prior to the deposition of the film. ZnO thin films with different thicknesses (8, 17, 28, and 58 nm) were coated on the as-prepared $LiCoO_2$ composite electrodes. The samples obtained were denoted as $LiCoO_2$/ZnO*x* (*x* = 8, 17, 28, and 58).

2.2. Materials Characterizations. The morphology was characterized by field-emission scanning electron microscope (FE-SEM, Hitachi, S3400N), and the compositions were analyzed with an energy dispersive X-ray spectroscope (EDS, Oxford INCA PentaFET-x3). The structure of the obtained electrode was characterized by X-ray diffraction using Cu Kα radiation (XRD, λ = 1.54056 Å, X'Pert Pro MPD) with a step size of 0.03° in the 2θ range of 10−80°. Raman spectra were obtained with a 532 nm wavelength laser (Renishaw, inVia Reflex).

2.3. Electrochemical Measurements. The electrochemical characterizations were conducted in two-electrode half cells. A Li foil was used as both the counter and reference electrodes. The traditionally fabricated $LiCoO_2$ porous composite electrode was prepared by spreading a mixture of $LiCoO_2$ powder, acetylene black, and polyvinylidene fluoride (PVDF, binder; 8:1:1 w/w) with *N*-methylpyrrolidone on a piece of Al foil. The cell was assembled in an Ar filled glovebox using lithium metal foil and a polypropylene (PP) membrane (Celgard 2400) as the counter electrode and the separator, respectively. A 1 mol L^{-1} $LiPF_6$ solution in a 1:1:1 (v/v/v) mixture of ethylene carbonate (EC), diethyl carbonate (DEC), and dimethyl carbonate (DMC) was used as the electrolyte. The charge−discharge curves were collected at desired current densities between 3.0 and 4.5 V by using a CT2001A cell test instrument (LAND Electronic Co.) at room temperature. Cyclic voltammograms (CV) were collected from 3.0 to 4.5 V at different scan rates using a Solartron SI1287 potentiostat.

3. RESULTS AND DISCUSSION

3.1. Physicochemical Characterization. The surface morphology and composition of bare $LiCoO_2$ and $LiCoO_2$/ZnO*x* electrodes were characterized by SEM and EDS, as shown in Figure 1. In the case of the bare $LiCoO_2$ composite electrode (Figure 1a), the $LiCoO_2$ particle sizes ranged from a few hundred nanometers to a few micrometers and were dispersed in a matrix of nanosized acetylene black conducting additives (average diameter around 30 nm). For the coated samples (Figure 1b,c), the amount of nanosized particles on the electrode surface increased with the extended deposition time. As the coating thickness increased to 58 nm (Figure 1d), the entire electrode surface was covered with agglomerated nanosized ZnO particles forming a continuous film. This trend was in line with the EDS results, where the peak intensity associated with Zn element increased with the layer thickness (Figure 1e). Additionally, the coating on the electrode surface was homogeneous, as was evident from the uniform distribution of Zn content in EDS mapping (Figure S1, Supporting Information). Note that the zinc oxide can also partly penetrate into the porous composite electrode as shown in its cross-sectional SEM and EDS (Figure 1f−h). The cobalt was uniformly distributed throughout the cross-section. On the contrary, the Zn element was concentrated in the vicinity of the electrode surface. Its concentration was far lower deeper in the electrode. Despite the weaker signal of Zn element, it was surprising to find that the spatial distribution of Zn element can

reach the interface between the composite electrode and the metallic current collector. This conformal coating is due to the porous structure offered by the composite electrode together with the high momentum of the sputtered species gained from high energy plasma.

The XRD patterns of bare and $LiCoO_2$/ZnO*x* electrodes are displayed in Figure 2. It can be seen that both bare $LiCoO_2$ and

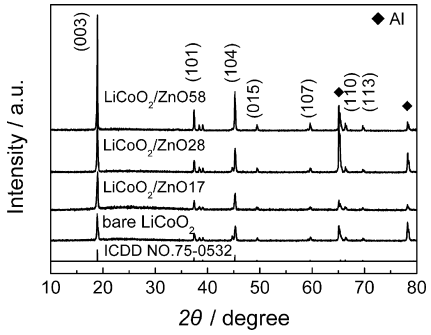

Figure 2. XRD patterns of bare $LiCoO_2$ and $LiCoO_2$/ZnO*x* electrodes, where the peaks in the XRD patterns match well with the standard α-$NaFeO_2$ structure (*R*3*m* space group) $LiCoO_2$ (ICDD No.75-0532).

$LiCoO_2$/ZnO*x* electrodes have a well-defined α-$NaFeO_2$ structure with the *R*3*m* space group. There was no shift of the diffraction peaks, which suggests that the ZnO coating does not cause any noticeable change in the crystal structure of $LiCoO_2$. Furthermore, there were no characteristic diffraction peaks of ZnO in these samples, even when the coating layer thickness approached 58 nm. Taking into account SEM results, it can be deduced that the deposited ZnO exists in an amorphous state.

3.2. Electrochemical Characterization. The cycling performance of the bare $LiCoO_2$ electrode and $LiCoO_2$/ZnO*x* electrodes between 3.0 and 4.5 V vs Li/Li^+ is displayed in Figure 3. Figure 3a shows the discharge capacities of the electrodes as a function of cycling number during galvanostatic charge−discharge tests. When the operation voltage window was enlarged from 3.0−4.2 V to 3.0−4.5 V, the initial discharge capacity of bare $LiCoO_2$ was elevated from ∼135 mAh g^{-1} to ∼193 mAh g^{-1} (Figure S2, Supporting Information). In the following cycles, however, the capacity of bare $LiCoO_2$ electrode quickly degraded to 140 mAh g^{-1} after 50 cycles, whereas the capacities of the ZnO-modified $LiCoO_2$ electrodes faded relatively slowly. It is also demonstrated that the capacity retention increased with increasing coating thickness up to 17 nm. From 17 nm up to the thickest film (58 nm) tested, the capacity decreased rapidly in the first 50 cycles. Among the electrodes tested, $LiCoO_2$/ZnO17 showed the best capacity retention. Its discharge capacity in the first cycle was as high as 191 mAh g^{-1}, and the reversible capacity was still 155 mAh g^{-1} after 200 cycles, with 0.09% decay per cycle. Figure 3b shows the capacity retention at the 50th cycle as a function of deposited ZnO thickness, where the capacity retention is taken to be the discharge capacity as a percentage of the initial discharge capacity. Compared with the capacity retention of 67.9% after 50 cycles for the bare $LiCoO_2$ electrode, the $LiCoO_2$/ZnO17 electrode retained 91.9% of its initial capacity. Further increasing the coating thickness resulted in a serious decay in capacity. Excess ZnO on the $LiCoO_2$ electrode surface could hinder Li-ion transport during the charge−discharge processes. The optimal thickness of the coating layer should keep the best balance between the electronic conductivity and the ionic conductivity.[7,38]

The electrochemical performance of bare and $LiCoO_2$/ZnO*x* electrodes cycled between 3.0 and 4.5 V at various C-rates is illustrated in Figure 4. At a current rate of 0.2 C (Figure 4a), the $LiCoO_2$/ZnO58 electrode shows slightly more polarization than the bare and $LiCoO_2$/ZnO17 electrodes in the initial charge profile, which could relate to the thicker coating layer that inhibits the lithium ion transportation. After the activation process and several cycles at 10 C without the help of coating, the bare electrode shows the worst capacity behavior and highest polarization (Figure 4b). This can be ascribed to the parasitic reaction with electrolyte and structural instability that commonly occur at the high oxidation state of $LiCoO_2$.[5,7] Among the electrodes tested, the $LiCoO_2$/ZnO17 electrode delivered the best rate performance. It showed a capacity of 191, 173, 156, 133, and 106 mAh g^{-1} at rates of 0.2, 1, 2, 4, and 10 C, respectively. When the rate was returned to 0.2 C after cycling at the higher rates, the capacity can be recovered to 174 mAh g^{-1}. At the highest C-rate of 10 C, the obtained discharge capacity of the $LiCoO_2$/ZnO17 electrode was 106 mAh g^{-1}, whereas the bare $LiCoO_2$ and $LiCoO_2$/ZnO58 showed only 75 and 82 mAh g^{-1}, respectively, under the same conditions. The rate performance of the ZnO-coated $LiCoO_2$ is quite good relative to that found in earlier work. It is even superior to the results of Jung et al.,[9] who were able to achieve a discharge capacity of 150 mAh g^{-1} at 1 C using Al_2O_3-coated $LiCoO_2$ prepared via an atomic layer deposition method.

Previous studies of $LiCoO_2$ electrodes claimed that the rapid deterioration of capacity during cycling is due to a hexagonal-monoclinic-hexagonal phase transition around 4.1 V.[18] To

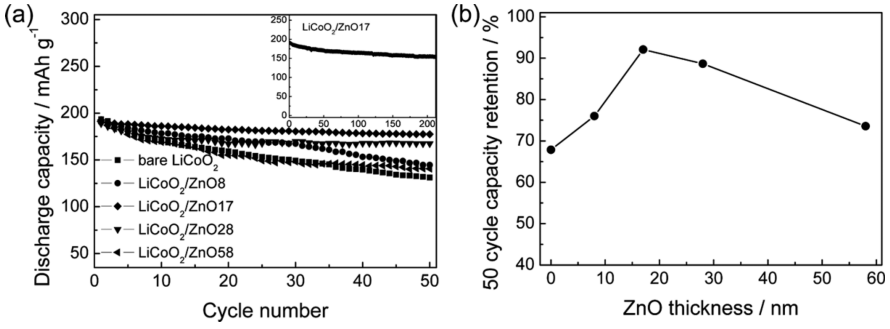

Figure 3. (a) Cyclic performance of the bare and $LiCoO_2$/ZnO*x* electrodes between 3.0 and 4.5 V at a rate of 0.2 C. (Inset) Long cycling performance of $LiCoO_2$/ZnO17 electrode at 0.2 C rate. (b) Capacity retention behavior of 50 cycles as a function of deposited ZnO thickness.

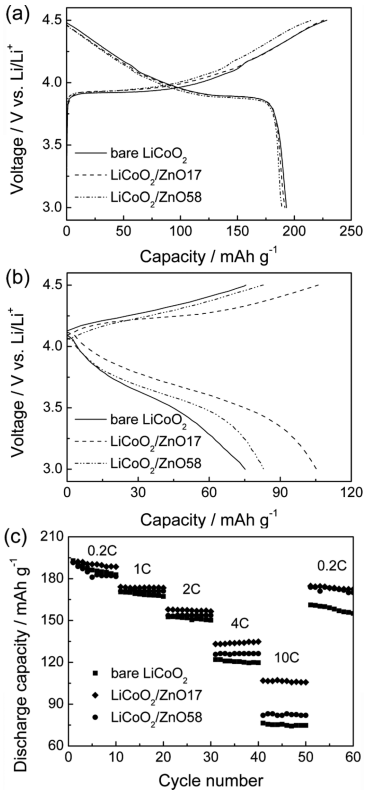

Figure 4. (a) Typical galvanostatic charge−discharge profiles of bare $LiCoO_2$ and $LiCoO_2$/ZnO*x* electrodes at 0.2 C, (b) galvanostatic charge−discharge profiles of bare $LiCoO_2$ and $LiCoO_2$/ZnO*x* electrodes at 10 C, (c) rate performance of bare $LiCoO_2$ and $LiCoO_2$/ZnO*x* electrodes at 0.2, 1, 2, 4, and 10 C, then returned to 0.2 C (with 1 C corresponding to 140 mA g^{-1}).

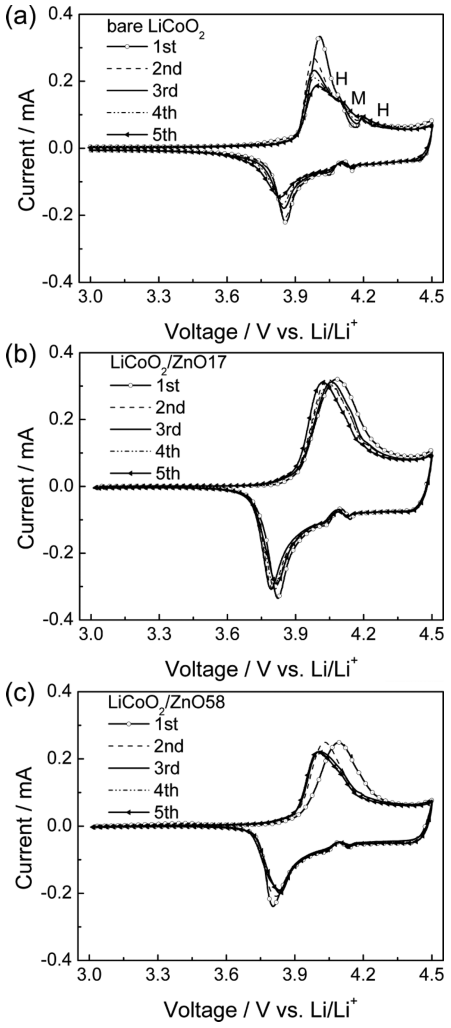

Figure 5. Cyclic voltammograms of (a) bare $LiCoO_2$, (b) $LiCoO_2$/ZnO17, and (c) $LiCoO_2$/ZnO58 electrodes at a scan rate of 0.05 mV s^{-1} between 3.0 and 4.5 V. H and M in (a) represent the hexagonal and monoclinic phase, respectively.

examine such a difference between bare and surface-coated $LiCoO_2$ electrodes upon cycling, we performed cyclic voltammograms for the bare and ZnO coated electrodes at a scan rate of 0.05 mV S^{1-} (Figure 5). There are clear differences in the peak intensities and positions of the redox reactions among these electrodes. Figure 5a shows that the characteristic voltammetric peaks corresponding to the phase transitions appear in every cycle for the bare $LiCoO_2$ electrode (H and M denote the hexagonal and monoclinic phases, respectively). For the $LiCoO_2$/ZnO*x* electrodes (Figure 5b,c), the voltammetric features associated with these phase transitions were suppressed in the positive-going sweep. Yoon et al.[39] reported that the (110) and (101) planes of $LiCoO_2$ have relatively high surface energies. The ZnO coating layer may preferentially deposit onto these planes.[40] These planes are almost perpendicular to the (003) plane. In this way, the coating layer can suppress the expansion of the *c* axis, and thus possibly lessen the degradation associated with this phase transition.[18,41] Furthermore, the coating of the high surface energy planes with a protective layer may prevent the parasitic reaction with electrolyte. It is known that the phase transition of hexagonal-monoclinic-hexagonal is the major cause of structural damage in $LiCoO_2$.[24,42] This implies that the $LiCoO_2$/ZnO*x* electrodes have better structural stability than the bare $LiCoO_2$ during charge and discharge, which will be further analyzed by XRD and Raman spectroscopy. Meanwhile, the peak currents and peak positions in the cyclic voltammograms of the $LiCoO_2$/ZnO*x* electrodes changed significantly less than those in the voltammogram of the bare $LiCoO_2$ electrode, providing further evidence of the improved stability of the coated electrodes and agreeing with the galvanostatic cycling data in Figure 3.

The bulk and surface structure information on the charged bare and $LiCoO_2$/ZnO*x* electrodes at 4.5 V after 50 cycles is presented in Figure 6. Compared with X-ray diffraction patterns of the $LiCoO_2$/ZnO*x* electrodes (Figure 6a), the (003) peak of the bare $LiCoO_2$ electrode displays a greater shift toward lower angles, which indicates an increase in the *c* axis length upon cycling.[3] Figure 6b shows the full width at half-maximum (fwhm) of (003) peak of bare and $LiCoO_2$/ZnO*x* electrodes before and after 50 cycles. It can be seen that the fwhm of (003) peak of the bare $LiCoO_2$ electrode increased rapidly after 50 cycles, whereas those of the $LiCoO_2$/ZnO*x* electrodes showed only a slight fwhm increase. Such peak broadening is due to structural degradation during cycling. Figure 6c,d shows the Raman spectra of bare and $LiCoO_2$/ZnO17 electrodes. Before cycling (Figure 6c), both the bare and ZnO-coated $LiCoO_2$ electrodes exhibited two characteristic bands near 482 and 593 cm^{-1}, respectively. According to previous studies,[43,44] these two bands can be assigned to the E_g (O−Co−O bending) and A_{1g} (Co−O stretching) Raman-active modes of the HT-$LiCoO_2$ phase. However, when measured at 4.5 V after 50 cycles between 3.0 and 4.5 V (Figure 6d), the bare $LiCoO_2$

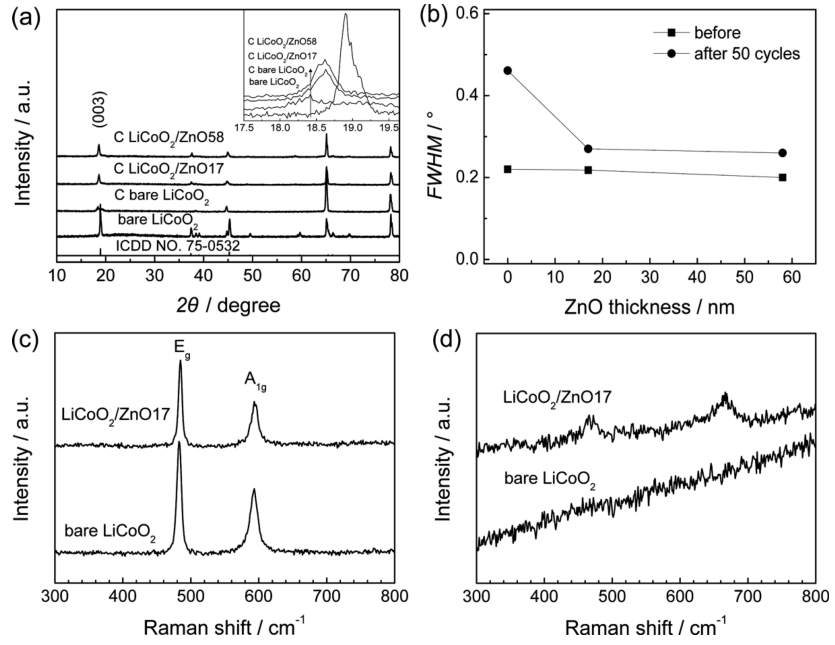

Figure 6. (a) XRD patterns of bare and $LiCoO_2/ZnOx$ electrodes charged to 4.5 V (C $LiCoO_2/ZnOx$) after 50 cycles between 3.0 and 4.5 V. Inset: enlarged (003) diffraction peaks. (b) fwhm of (003) peak of bare $LiCoO_2$ and $LiCoO_2/ZnOx$ electrodes before cycling and after 50 cycles. Raman spectra of bare $LiCoO_2$ and $LiCoO_2$/ZnO17 electrode (c) at an initial state and (d) after 50th cycle at 4.5 V.

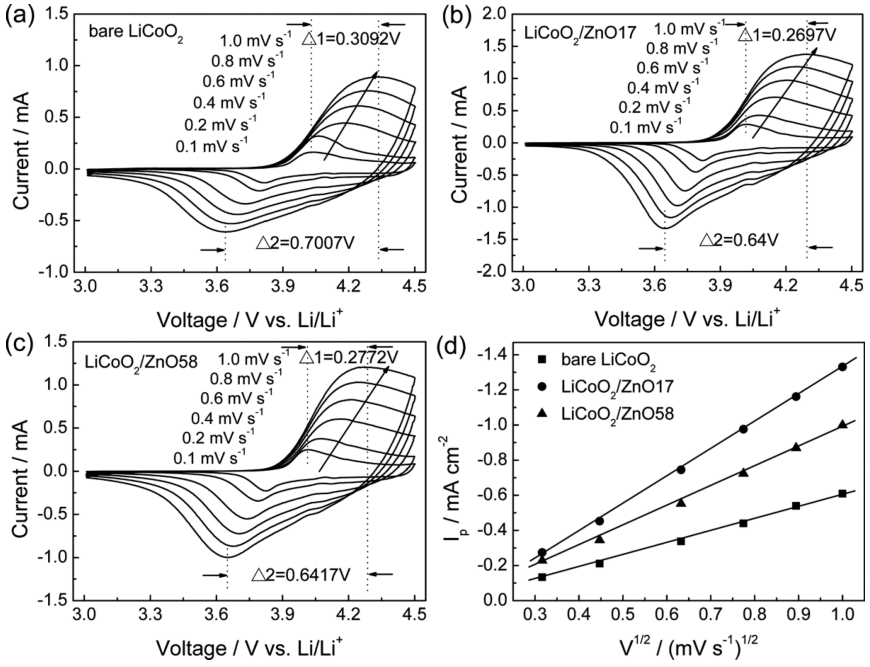

Figure 7. Cyclic voltammograms of (a) bare $LiCoO_2$, (b) $LiCoO_2$/ZnO17, and (c) $LiCoO_2$/ZnO58 electrodes were carried out between 3.0 and 4.5 V over a scan rate of 0.1−1.0 mV s^{-1} after a formation cycle; Δ1 denotes the difference of anodic peaks between 0.1 and 1.0 mV s^{-1}, and Δ2 denotes the difference of redox peaks for 1.0 mV s^{-1}. (d) Peak current against square root of scan rate for these three electrodes.

electrode did not show any noticeable Raman signal. In contrast, the $LiCoO_2$/ZnO17 electrode revealed an intensity-weakened E_g mode and nanostructure compound Co_3O_4 near 675 cm^{-1}.[45,46] These results demonstrate that the bare $LiCoO_2$ electrode had more severe structural and surface changes than did the $LiCoO_2$/ZnO17 electrode after 50 cycles. These results provide concrete evidence for the effect of ZnO coating on improving the structural stability and surface stability of $LiCoO_2$ during cycling.

To investigate the influence of ZnO coating layer on the kinetic performance of $LiCoO_2$, we collected CV experiments of the bare $LiCoO_2$ and $LiCoO_2/ZnOx$ electrodes over a range of scan rates from 0.1 to 1.0 mV s^{-1} (Figure 7). They revealed that the peak current (I_p) increased with increasing scan rate, while the anodic peaks shifted to higher potential, and the cathodic peaks shifted to lower potential. Moreover, the value of Δ1 and Δ2 (Δ1 denotes the voltage difference of anodic peaks between 0.1 and 1.0 mV s^{-1}, and Δ2 denotes the potential difference between the anodic and cathodic peaks at

1.0 mV s^{-1}, as shown in Figure 7a–c) for the $LiCoO_2$/ZnO17 electrode was smaller than that for both the bare $LiCoO_2$ and $LiCoO_2$/ZnO58 electrodes. Thus, it can be easily deduced that the 17 nm thick ZnO-coated $LiCoO_2$ electrode polarized less than the other electrodes. Figure 7d shows the correlation between the cathodic peak currents and the square root of the scan rate ($v^{1/2}$) for these $LiCoO_2$-based electrodes, which matches the linear relationship very well. It is a typical behavior of diffusion-controlled process. Therefore, the Li-ion diffusion coefficient in the electrodes could be estimated by using Randles–Sevcik relation, which is expressed as[47,48]

$$I_p = 0.4463 n^{3/2} F^{3/2} C_{Li} S R^{-1/2} T^{-1/2} \tilde{D}_{Li}^{1/2} \nu^{1/2} \quad (1)$$

where I_p is the peak current (A), n is the number of electrons transferred, F is the Faraday constant (96485.4 C mol^{-1}), C_{Li} is the Li-ion concentration (0.051 mol cm^{-3}), S is the surface area in cm^2 of the electrode, R is the gas constant (8.314 J mol^{-1} K^{-1}), T is the absolute temperature (K), $\tilde{D}_{Li}$ and v are Li-ion chemical diffusion coefficient (cm^2 s^{-1}) and scan rate (V s^{-1}), respectively. Based on eq 1, the apparent diffusion coefficients of Li-ion for bare $LiCoO_2$, $LiCoO_2$/ZnO17, and $LiCoO_2$/ZnO58 are 3.95×10^{-12}, 1.88×10^{-11}, and 1.00×10^{-11} cm^2 s^{-1}, respectively. It is obvious that the $LiCoO_2$/ZnO17 sample has the highest Li-ion diffusion coefficient, while the bare $LiCoO_2$ electrode has the lowest Li-ion diffusion coefficient. To explain this, two factors should be taken into consideration: First, the ZnO coating improves the structural stability of $LiCoO_2$. Second, the ZnO coating suppresses the formation of passivating films on the $LiCoO_2$ surfaces. A too-thick ZnO layer on the surface of the $LiCoO_2$ electrode can also inhibit the Li-ion transport across the interface between the surface layer and electrode.

4. CONCLUSIONS

Deposition of a conformal ZnO film on as-prepared $LiCoO_2$ electrode via RF magnetron sputtering is an effective way to improve its electrochemical performance of $LiCoO_2$ at high cutoff voltages. The ZnO-coated $LiCoO_2$ with an optimum coating thickness of 17 nm showed an initial discharge capacity of 191 mAh g^{-1} and capacity retention of more than 81% after 200 cycles at 0.2 C. It achieved a discharge capacity of 106 mAh g^{-1} at 10 C. The electrochemical performance improved in terms of capacity, capacity retention, and rate performance was ascribed to the better electronic transport pathways supported by the as-prepared electrode, a more stable structure and higher lithium ion chemical diffusion coefficient assisted by the coating of ZnO film. RF magnetron sputtering of oxide films directly onto as-prepared electrodes can be broadened to other electrode materials.

■ ASSOCIATED CONTENT

Supporting Information

Surface SEM images and corresponding EDS maps for elements Co and Zn of $LiCoO_2$/ZnO17. Charge–discharge curves of bare $LiCoO_2$ between 3.0–4.2 V and 3.0–4.5 V at 0.2 C. This material is available free of charge via the Internet at http://pubs.acs.org.

■ AUTHOR INFORMATION

Corresponding Authors

*E-mail: lijingze@uestc.edu.cn. Tel.: +86 28 83207620. Fax: +86 28 83202569.

*E-mail: lipingwang@uestc.edu.cn. Tel.: +86 28 83207620. Fax: +86 28 83202569.

Notes

The authors declare no competing financial interest.

■ ACKNOWLEDGMENTS

This work was supported in part by the National Natural Science Foundation of China (Nos. 21473022, 51033006, 51102039, 51211140045, and 11234013), the Fundamental Research Funds for the Central Universities (Nos. ZYGX2012Z003 and ZYGX2010J033) and the China Postdoctoral Science Foundation (Nos. 20100481375 and 201104640). We would like to thank Dr. Eric Rus (Brookhaven National Laboratory, Upton, NY) for English improvement and fruitful discussions.

■ REFERENCES

(1) Amatucci, G.; Tarascon, J.; Klein, L. Cobalt Dissolution in $LiCoO_2$-Based Non-Aqueous Rechargeable Batteries. *Solid State Ionics* **1996**, *83*, 167–173.

(2) Wang, H.; Jang, Y. I.; Huang, B.; Sadoway, D. R.; Chiang, Y. M. TEM Study of Electrochemical Cycling-Induced Damage and Disorder in $LiCoO_2$ Cathodes for Rechargeable Lithium Batteries. *J. Electrochem. Soc.* **1999**, *146*, 473–480.

(3) Reimers, J. N.; Dahn, J. Electrochemical and in Situ X-ray Diffraction Studies of Lithium Intercalation in Li_xCoO_2. *J. Electrochem. Soc.* **1992**, *139*, 2091–2097.

(4) Bai, Y.; Shi, H.; Wang, Z.; Chen, L. Performance Improvement of $LiCoO_2$ by Molten Salt Surface Modification. *J. Power Sources* **2007**, *167*, 504–509.

(5) Chen, Z. H.; Dahn, J. R. Methods to Obtain Excellent Capacity Retention in $LiCoO_2$ Cycled to 4.5 V. *Electrochim. Acta* **2004**, *49*, 1079–1090.

(6) Aurbach, D.; Markovsky, B.; Rodkin, A.; Levi, E.; Cohen, Y. S.; Kim, H. J.; Schmidt, M. On the Capacity Fading of $LiCoO_2$ Intercalation Electrodes: The Effect of Cycling, Storage, Temperature, and Surface Film Forming Additives. *Electrochim. Acta* **2002**, *47*, 4291–4306.

(7) Chang, W.; Choi, J. W.; Im, J. C.; Lee, J. K. Effects of ZnO Coating on Electrochemical Performance and Thermal Stability of $LiCoO_2$ as Cathode Material for Lithium-Ion Batteries. *J. Power Sources* **2010**, *195*, 320–326.

(8) Cho, J.; Kim, G. B.; Lim, H. S.; Kim, C. S.; Yoo, S. I. Improvement of Structural Stability of $LiMn_2O_4$ Cathode Material on 55 °C Cycling by Sol-Gel Coating of $LiCoO_2$. *Electrochem. Solid-State Lett.* **1999**, *2*, 607–609.

(9) Jung, Y. S.; Cavanagh, A. S.; Riley, L. A.; Kang, S. H.; Dillon, A. C.; Groner, M. D.; George, S. M.; Lee, S. H. Ultrathin Direct Atomic Layer Deposition on Composite Electrodes for Highly Durable and Safe Li-Ion Batteries. *Adv. Mater.* **2010**, *22*, 2172–2176.

(10) Choi, K. H.; Jeon, J. H.; Park, H. K.; Lee, S. M. Electrochemical Performance and Thermal Stability of $LiCoO_2$ Cathodes Surface-Modified with a Sputtered Thin Film of Lithium Phosphorus Oxynitride. *J. Power Sources* **2010**, *195*, 8317–8321.

(11) Cao, Q.; Zhang, H. P.; Wang, G. J.; Xia, Q.; Wu, Y. P.; Wu, H. Q. A Novel Carbon-Coated $LiCoO_2$ as Cathode Material for Lithium Ion Battery. *Electrochem. Commun.* **2007**, *9*, 1228–1232.

(12) Scott, I. D.; Jung, Y. S.; Cavanagh, A. S.; An, Y.; Dillon, A. C.; George, S. M.; Lee, S. H. Ultrathin Coatings on Nano-$LiCoO_2$ for Li-Ion Vehicular Applications. *Nano Lett.* **2011**, *11*, 414–418.

(13) Yoon, W. S.; Lee, K. K.; Kim, K. B. Synthesis of $LiAl_{(y)}Co_{(1-y)}O_{(2)}$ Using Acrylic Acid and Its Electrochemical Properties for Li Rechargeable Batteries. *J. Power Sources* **2001**, *97–98*, 303–307.

(14) Ceder, G.; Chiang, Y. M.; Sadoway, D.; Aydinol, M.; Jang, Y. I.; Huang, B. Identification of Cathode Materials for Lithium Batteries Guided by First-Principles Calculations. *Nature* **1998**, *392*, 694–696.

(15) Valanarasu, S.; Chandramohan, R.; Thirumalai, J.; Vijayan, T. A. Structural and Electrochemical Investigation of Zn-Doped $LiCoO_2$ Powders. *Ionics* **2012**, *18*, 39−45.
(16) Nithya, C.; Thirunakaran, R.; Sivashanmugam, A.; Gopukumar, S. High-Performing $LiMg_xCu_yCo_{1-x-y}O_2$ Cathode Material for Lithium Rechargeable Batteries. *ACS Appl. Mater. Interfaces* **2012**, *4*, 4040−4046.
(17) Kobayashi, H.; Shigemura, H.; Tabuchi, M.; Sakaebe, H.; Ado, K.; Kageyama, H.; Hirano, A.; Kanno, R.; Wakita, M.; Morimoto, S. Electrochemical Properties of Hydrothermally Obtained $LiCo_{1-x}Fe_xO_2$ as a Positive Electrode Material for Rechargeable Lithium Batteries. *J. Electrochem. Soc.* **2000**, *147*, 960−969.
(18) Cho, J.; Kim, Y. J.; Park, B. Novel $LiCoO_2$ Cathode Material with Al_2O_3 Coating for a Li Ion Cell. *Chem. Mater.* **2000**, *12*, 3788−3791.
(19) Wang, Z. X.; Liu, L. J.; Chen, L. Q.; Huang, X. J. Structural and Electrochemical Characterizations of Surface-Modified $LiCoO_2$ Cathode Materials for Li-Ion Batteries. *Solid State Ionics* **2002**, *148*, 335−342.
(20) Fang, T.; Duh, J. G.; Sheen, S. R. Improving the Electrochemical Performance of $LiCoO_2$ Cathode by Nanocrystalline ZnO Coating. *J. Electrochem. Soc.* **2005**, *152*, A1701−A1706.
(21) Cho, J.; Kim, Y. J.; Kim, T. J.; Park, B. Zero-Strain Intercalation Cathode for Rechargeable Li-Ion Cell. *Angew. Chem., Int. Ed.* **2001**, *40*, 3367−3369.
(22) Hwang, B. J.; Chen, C. Y.; Cheng, M. Y.; Santhanam, R.; Ragavendran, K. Mechanism Study of Enhanced Electrochemical Performance of ZrO_2-Coated $LiCoO_2$ in High Voltage Region. *J. Power Sources* **2010**, *195*, 4255−4265.
(23) Wang, Z. X.; Wu, C. A.; Liu, L. J.; Wu, F.; Chen, L. Q.; Huang, X. J. Electrochemical Evaluation and Structural Characterization of Commercial $LiCoO_2$ Surfaces Modified with MgO for Lithium-Ion Batteries. *J. Electrochem. Soc.* **2002**, *149*, A466−A471.
(24) Cho, J.; Kim, C. S.; Yoo, S. I. Improvement of Structural Stability of $LiCoO_2$ Cathode during Electrochemical Cycling by Sol-Gel Coating of SnO_2. *Electrochem. Solid-State Lett.* **2000**, *3*, 362−365.
(25) Tian, S.; Liu, L. L.; Zhu, Y. S.; Hou, Y. Y.; Hu, C. L.; Wu, Y. P. Improving Electrochemical Performance of $LiCoO_2$ by TiO_2 Coating as Cathode for Aqueous Rechargeable Lithium Batteries. *Funct. Mater. Lett.* **2013**, *6*, 1350016.
(26) Cho, J.; Lee, J. G.; Kim, B.; Park, B. Effect of P_2O_5 and $AlPO_4$ Coating on $LiCoO_2$ Cathode Material. *Chem. Mater.* **2003**, *15*, 3190−3193.
(27) Wu, Z. S.; Xue, L.; Ren, W.; Li, F.; Wen, L.; Cheng, H. M. A LiF Nanoparticle-Modified Graphene Electrode for High-Power and High-Energy Lithium Ion Batteries. *Adv. Funct. Mater.* **2012**, *22*, 3290−3297.
(28) Murakami, M.; Yamashige, H.; Arai, H.; Uchimoto, Y.; Ogumi, Z. Association of Paramagnetic Species with Formation of LiF at the Surface of $LiCoO_2$. *Electrochim. Acta* **2012**, *78*, 49−54.
(29) Lee, H. J.; Park, Y. J. Interface Characterization of MgF_2-Coated $LiCoO_2$ Thin Films. *Solid State Ionics* **2013**, *230*, 86−91.
(30) Park, S. B.; Shin, H. C.; Lee, W. G.; Cho, W. I.; Jang, H. Improvement of Capacity Fading Resistance of $LiMn_2O_4$ by Amphoteric Oxides. *J. Power Sources* **2008**, *180*, 597−601.
(31) Moon, S. M.; Chang, W.; Byun, D.; Lee, J. K. Comparative Studies on ZnO-Coated and Uncoated $LiCoO_2$ Cycled at Various Rates and Temperatures. *Curr. Appl. Phys.* **2010**, *10*, E122−E126.
(32) Bettge, M.; Li, Y.; Sankaran, B.; Rago, N. D.; Spila, T.; Haasch, R. T.; Petrov, I.; Abraham, D. P. Improving High-Capacity $Li_{1.2}Ni_{0.15}Mn_{0.55}Co_{0.1}O_2$-based Lithium-Ion Cells by Modifiying the Positive Electrode with Alumina. *J. Power Sources* **2013**, *233*, 346−357.
(33) Zhao, J.; Wang, Y. Ultrathin Surface Coatings for Improved Electrochemical Performance of Lithium Ion Battery Electrodes at Elevated Temperature. *J. Phys. Chem. C* **2012**, *116*, 11867−11876.
(34) Jung, Y. S.; Lu, P.; Cavanagh, A. S.; Ban, C.; Kim, G. H.; Lee, S. H.; George, S. M.; Harris, S. J.; Dillon, A. C. Unexpected Improved Performance of ALD Coated $LiCoO_2$/Graphite Li-Ion Batteries. *Adv. Energy Mater.* **2013**, *3*, 213−219.
(35) Tan, G.; Wu, F.; Li, L.; Chen, R.; Chen, S. Coralline Glassy Lithium Phosphate-Coated $LiFePO_4$ Cathodes with Improved Power Capability for Lithium Ion Batteries. *J. Phys. Chem. C* **2013**, *117*, 6013−6021.
(36) Kang, E.; Jung, Y. S.; Cavanagh, A. S.; Kim, G. H.; George, S. M.; Dillon, A. C.; Kim, J. K.; Lee, J. Fe_3O_4 Nanoparticles Confined in Mesocellular Carbon Foam for High Performance Anode Materials for Lithium-Ion Batteries. *Adv. Funct. Mater.* **2011**, *21*, 2430−2438.
(37) Meng, X.; Yang, X. Q.; Sun, X. Emerging Applications of Atomic Layer Deposition for Lithium-Ion Battery Studies. *Adv. Mater.* **2012**, *24*, 3589−3615.
(38) Zhang, H.; Deng, Q.; Mou, C.; Huang, Z.; Wang, Y.; Zhou, A.; Li, J. Surface Structure and High-Rate Performance of Spinel $Li_4Ti_5O_{12}$ Coated with N-Doped Carbon as Anode Material for Lithium-Ion Batteries. *J. Power Sources* **2013**, *239*, 538−545.
(39) Yoon, Y.; Park, C.; Kim, J.; Shin, D. Lattice Orientation Control of Lithium Cobalt Oxide Cathode Film for All-Solid-State Thin Film Batteries. *J. Power Sources* **2013**, *226*, 186−190.
(40) Fang, T.; Duh, J. G. Effect of Calcination Temperature on the Electrochemical Behavior of ZnO-Coated $LiCoO_2$ Cathode. *Surf. Coat. Technol.* **2006**, *201*, 1886−1893.
(41) Kim, Y. J.; Kim, T. J.; Shin, J. W.; Park, B.; Cho, J. The Effect of Al_2O_3 Coating on the Cycle Life Performance in Thin-Film $LiCoO_2$ Cathodes. *J. Electrochem. Soc.* **2002**, *149*, A1337−A1341.
(42) Amatucci, G.; Tarascon, J.; Klein, L. CoO_2, The End Member of the Li_xCoO_2 Solid Solution. *J. Electrochem. Soc.* **1996**, *143*, 1114−1123.
(43) Huang, W.; Frech, R. Vibrational, Spectroscopic, and Electrochemical Studies of the Low and High Temperature Phases of $LiCo_{1-x}M_xO_2$ (M = Ni or Ti). *Solid State Ionics* **1996**, *86*, 395−400.
(44) Porthault, H.; Baddour-Hadjean, R.; Le Cras, F.; Bourbon, C.; Franger, S. Raman Study of the Spinel-to-Layered Phase Transformation in Sol-Gel $LiCoO_2$ Cathode Powders as a Function of the Post-Annealing Temperature. *Vib. Spectrosc.* **2012**, *62*, 152−158.
(45) Burba, C. M.; Shaju, K. M.; Bruce, P. G.; Frech, R. Infrared and Raman Spectroscopy of Nanostructured LT-$LiCoO_2$ Cathodes for Li-Ion Rechargeable Batteries. *Vib. Spectrosc.* **2009**, *51*, 248−250.
(46) Park, Y.; Kim, N. H.; Kim, J. Y.; Eom, I. Y.; Jeong, Y. U.; Kim, M. S.; Lee, S. M.; Choi, H. C.; Jung, Y. M. Surface Characterization of the High Voltage $LiCoO_2$/Li Cell by X-ray Photoelectron Spectroscopy and 2D Correlation Analysis. *Vib. Spectrosc.* **2010**, *53*, 60−63.
(47) Tang, S.; Lai, M.; Lu, L. Li-Ion Diffusion in Highly (003) Oriented $LiCoO_2$ Thin Film Cathode Prepared by Pulsed Laser Deposition. *J. Alloys Compd.* **2008**, *449*, 300−303.
(48) Xie, J.; Imanishi, N.; Matsumura, T.; Hirano, A.; Takeda, Y.; Yamamoto, O. Orientation Dependence of Li-Ion Diffusion Kinetics in $LiCoO_2$ Thin Films Prepared by RF Magnetron Sputtering. *Solid State Ionics* **2008**, *179*, 362−370.